

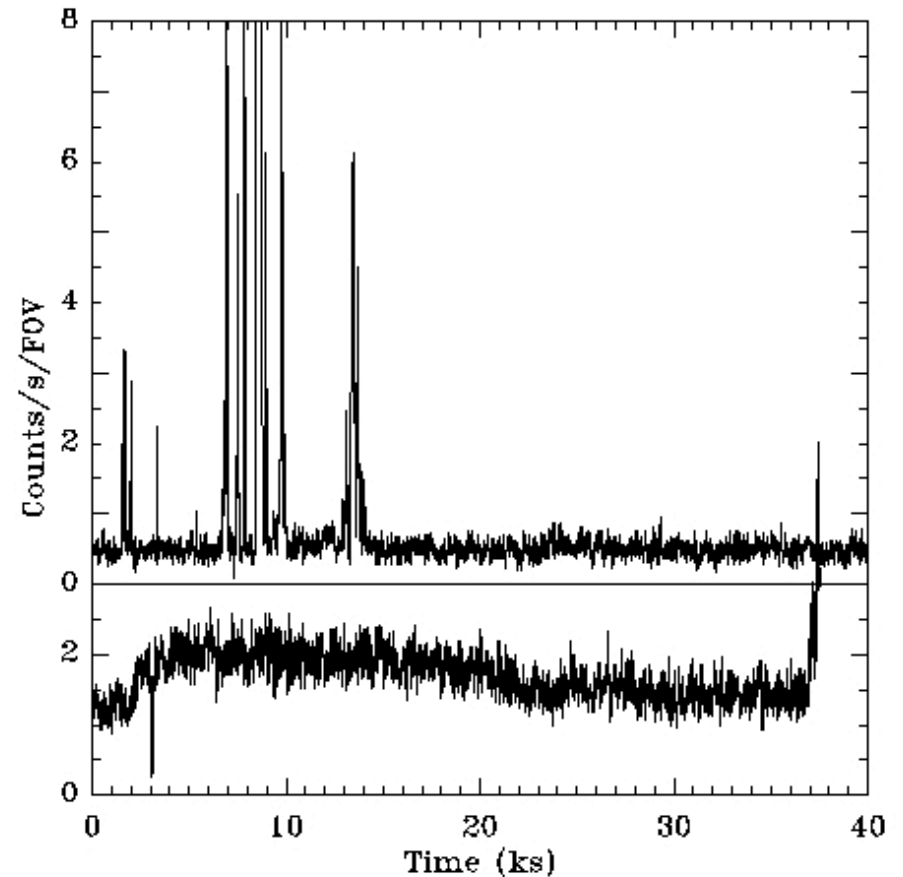
Why are the Soft Proton Flares  
Such a Problem for XMM,  
Not a (significant) problem for  
Chandra, and  
Is there anything to be done  
about them?

**K.D.Kuntz, B. Walsh,**  
M. Collier, B. Perry, D. Sibeck, S. Snowden

# Setting the Problem

## Soft Proton Flares (SPF)

- increase backgrounds by XXX
- duration scales: 10 s —  $10^4$  s
- variable at many frequencies
- not be detectable in short exp.
- affect 51% of exposure time



## Soft Proton Flares (SPF)

- allow study of the lower energy population of energetic particles
- (and people who study such things are interested)

## FLARING COMPONENT

- PAT 0-4 ONLY  $\Rightarrow$  CONV. NEAR SURFACE OF CCD  
PAT 31 NOT SEEN
- WHEN PRESENT, THE TOTAL BKG. INTENS. CAN INCREASE BY ORDERS OF MAGNITUDE
- SPECTRUM IS HARD (MEAS. IN LOW GAIN)
- FLARES ARE NOT SEEN IN RADIATION MONITOR (SHOULD BE IF PARTICLES WERE LOW ENERGY ( $E \approx 50$  keV) ELECTRONS)
- ENERGY LOSS THROUGH FILTERS IS CONSISTENT WITH EXPECTATIONS FOR SOFT PROTONS, ( $E \approx 200$  keV)
- PARTICLES ENTER THROUGH TELESCOPE VIGNETTING IS SEEN IN ALL 3 UNITS
- LOW EN. ELECTRONS SHOULD BE REMOVED FROM MAGNETIC DEFL.

FLARES ARE DUE TO  
SOFT PROTONS.

## SOFT PROTONS

WHERE DO THEY COME FROM?

FLARES ARE SPATIALLY LOCALIZED AND TYPICALLY AWAY FROM APOGEE.

REPETITION OF L.C. STRUCTURE FROM REV 70 TO 71 IS NOT PERFECT.

MOS1 & MOS2 BEHAVIOUR IS ALMOST IDENTICAL.

FLARES ARE MOST LIKELY STRUCTURED IN CLOUDS WHICH ARE SLOWLY MOVING THROUGH THE MAGNETOSP.

S.P. ARE MOST LIKELY STRUCTURED IN CLOUDS WHICH ARE SLOWLY MOVING THROUGH THE MAGNETOSP.

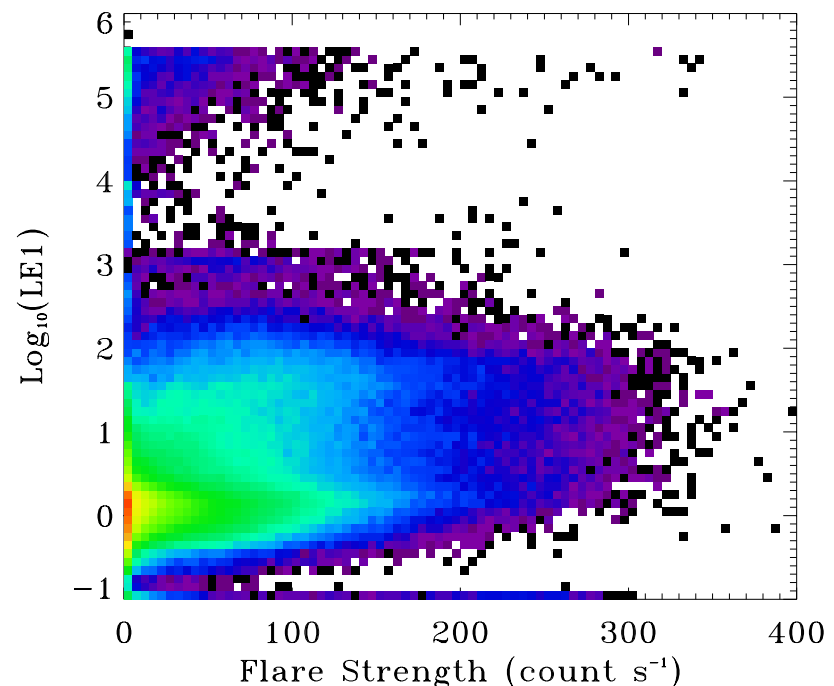
Silvano Molendi ca. 2000

# Summary of Standard Wisdom

Background flares are due to “soft” protons

- from XMM patterns - deposit energy near surface → low E
- sweeping magnets
  - remove  $e^-$  below 20 keV and
  - reduce by  $\sim 10^5$   $e^-$  in 20 keV-100 keV range
- not correlated with EPIC Radiation Monitor (ERM) measures
  - thus not these particles in these Energy Ranges
- modulated by filters
- vignettted

	$e^-$	$p^+$
LE	0.13-1.5 MeV	1.0-4.5 MeV
HE	1.0-1.75MeV	8-40 MeV



# Filter Modulation

Each MOS camera has identical filter sets:

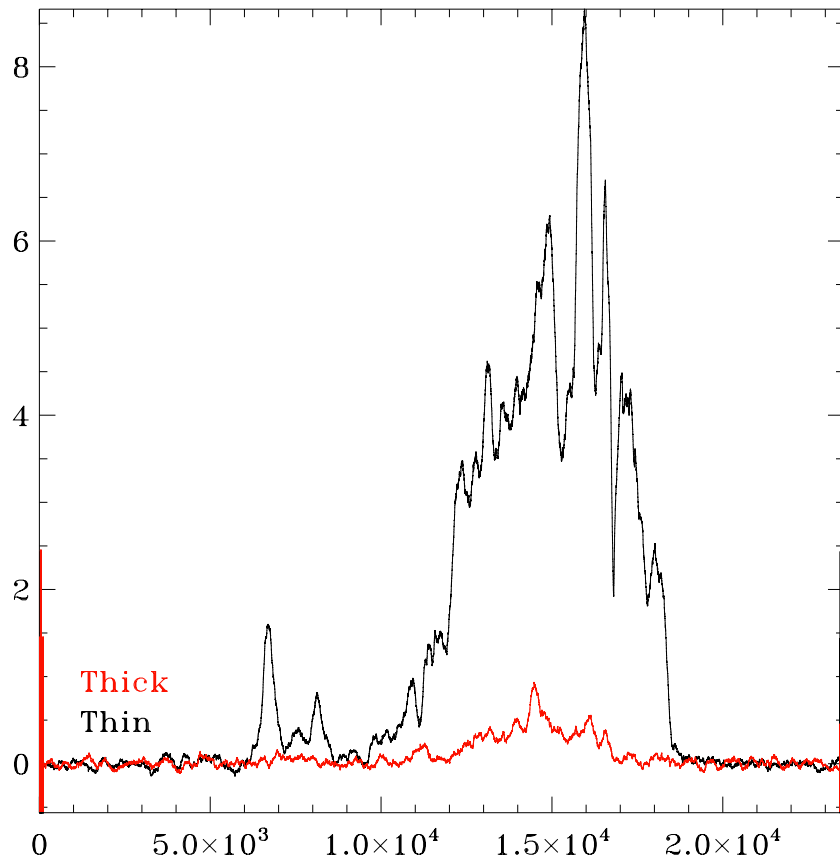
Filter	polyimide	Al	Sn	Stopping Power (100 keV)
Thin	160 nm	40 nm		8 keV
Medium	160 nm	800 nm		100 keV
Thick	330 nm	160 nm	40 nm	59 keV

Stopping power calculations were very roughly done.

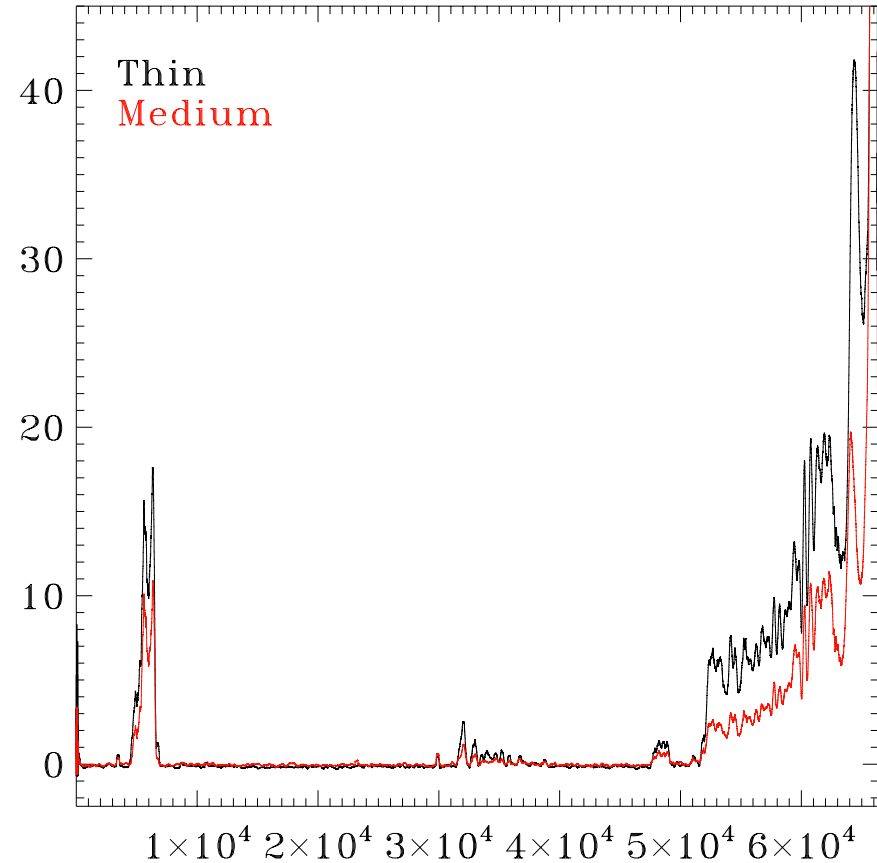
Expect reduction of 6-12X between Thin and the other filters

# Filter Modulation

0102040201



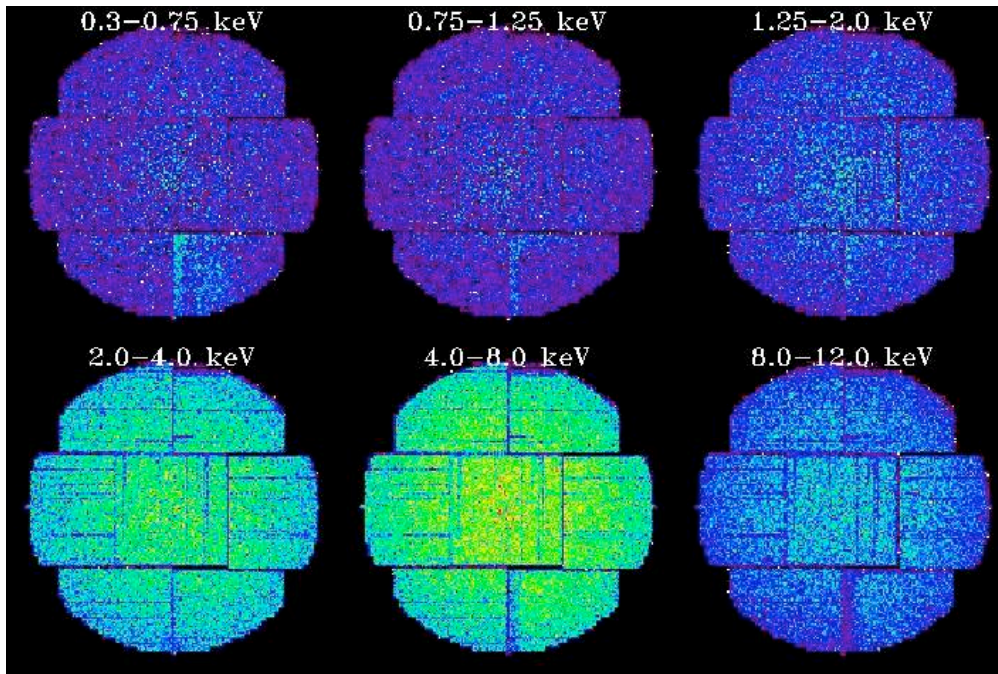
0109660801



## Two examples

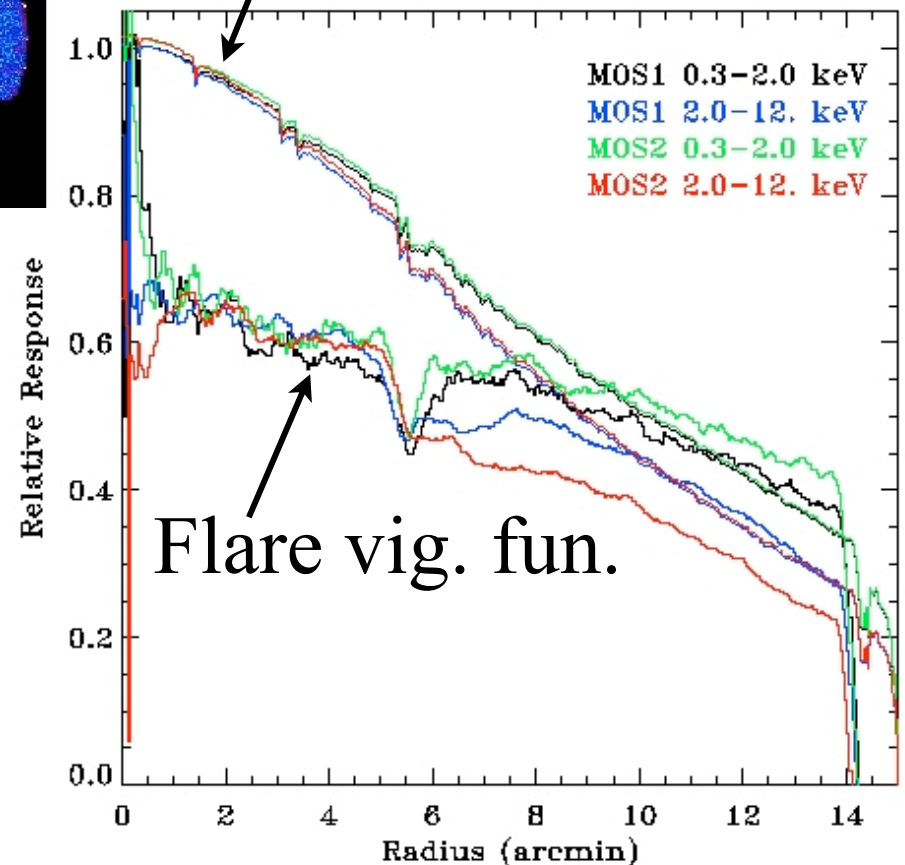
- filter to filter ratios vary with time (thus  $p^+$  energies varying)
- ratios aren't quite those expected - but in the right range

# Vignetting



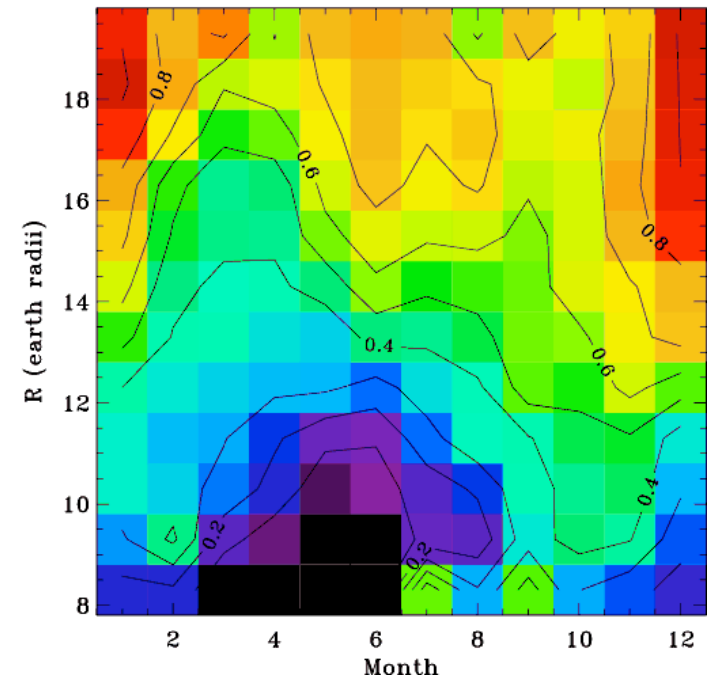
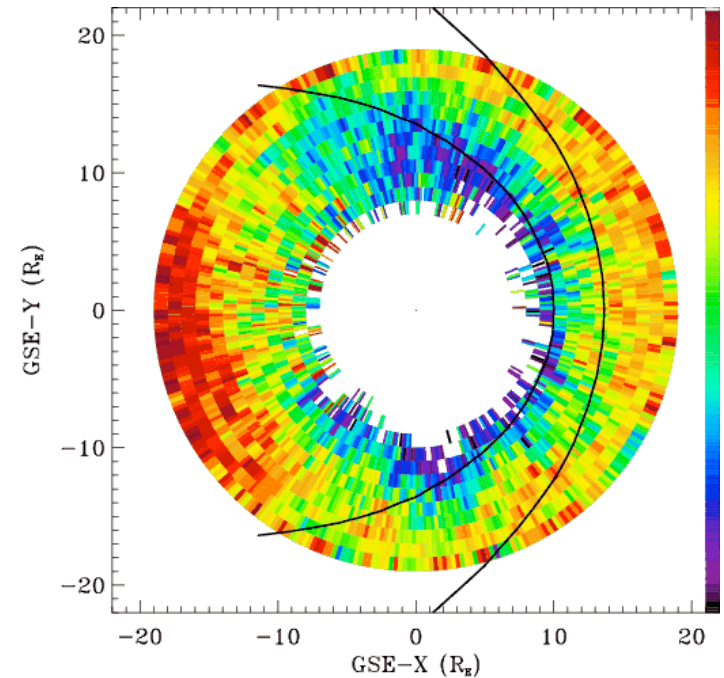
Vignetting  $\rightarrow$  particles  
interaction with the mirrors  
Flare vignetting measured for  
use in XMM-ESAS as  $f(E)$

Photon vig. fun.



# Old News

- SPF are worse closer to the Earth
- no orbit-to-orbit repetition
- SPF occur preferentially at certain times of year (Kuntz & Snowden 2008)
  - soft protons related to particular parts of the magnetosheath
  - the magnetopause particularly problematic
- Tools too crude to go further

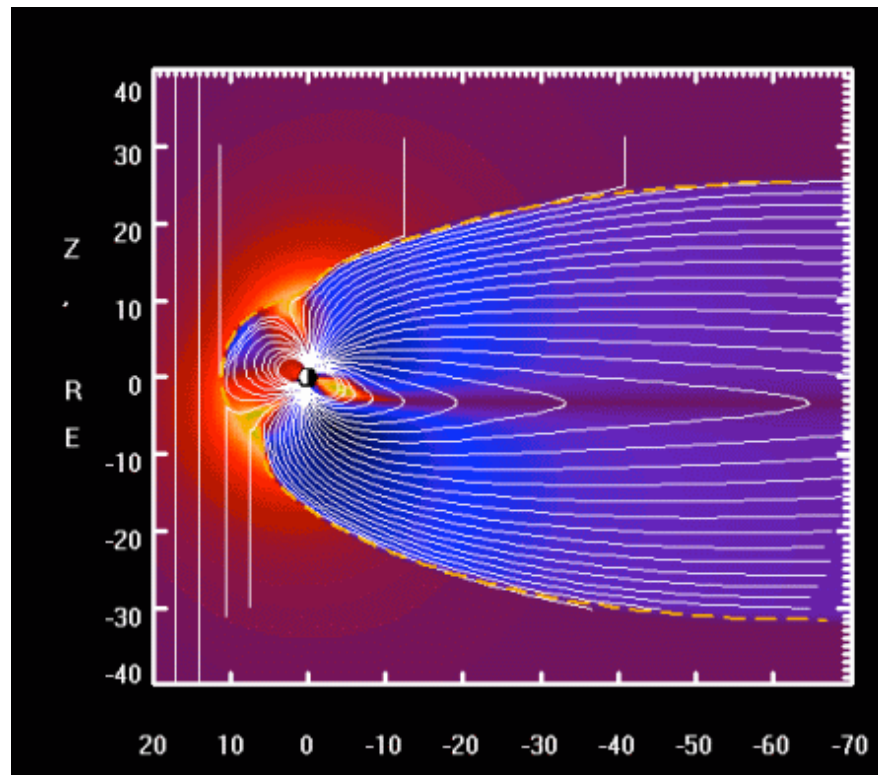


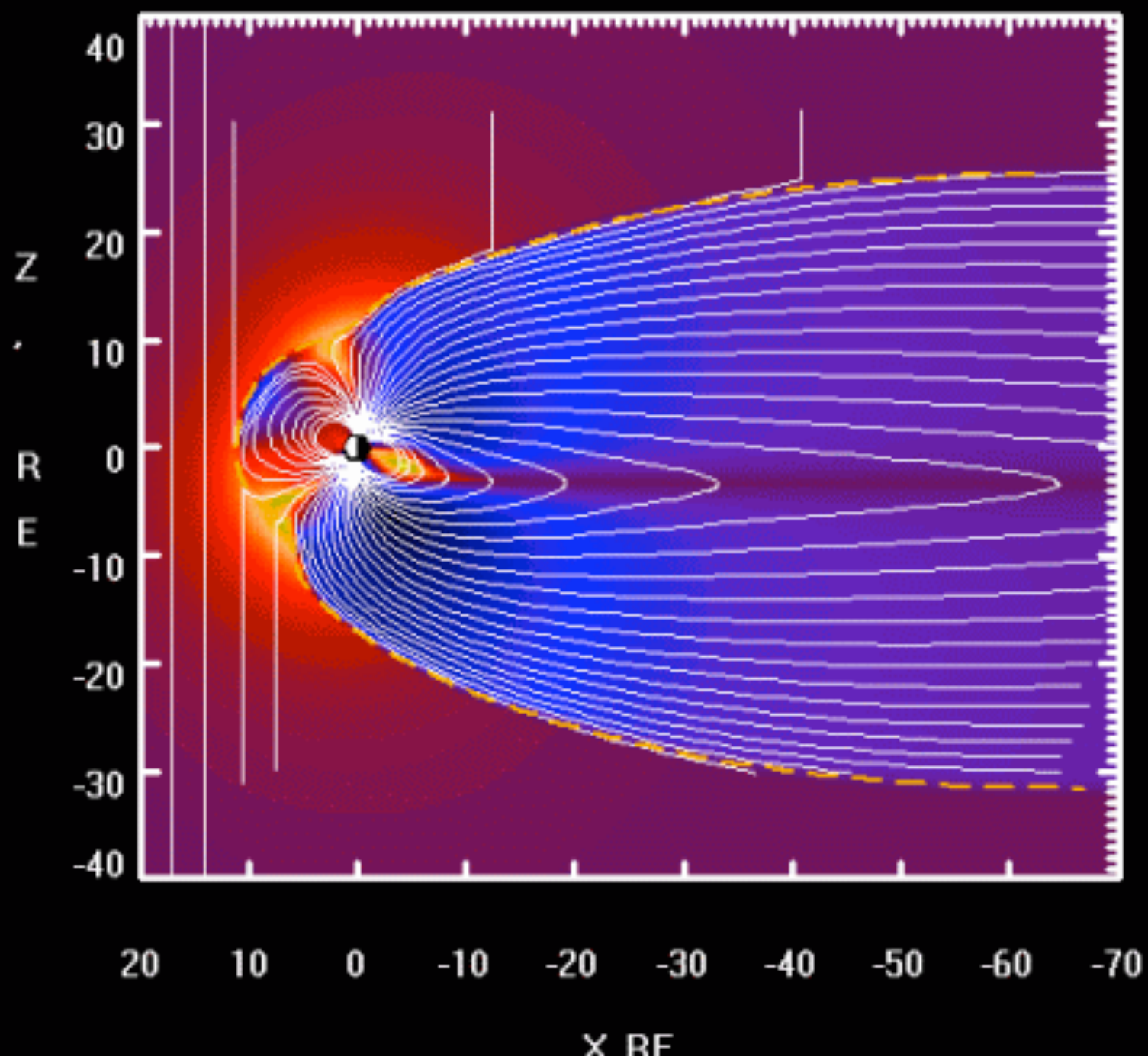


# Renewed Efforts

- The XMM Trend data
  - contains flare data, spacecraft data, solar wind data
  - aligned to the same time steps
  - currently being upgraded (again)
- (Acceptable) model of the Earth's B field
  - depends on solar wind flux and IMF
  - allows one to determine local field geometry

Nikolai Tsyganenko

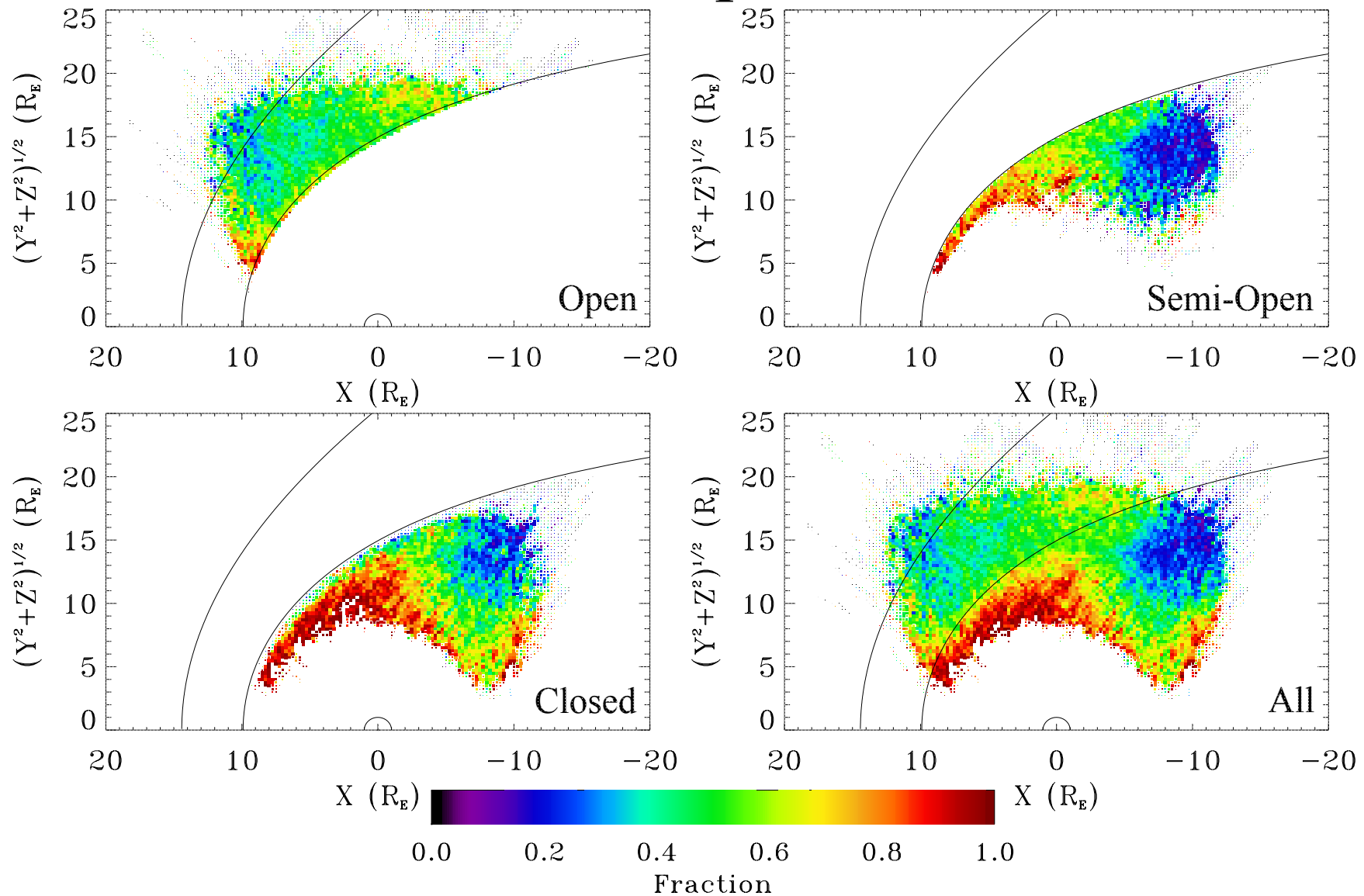




# Renewed Efforts

- Reconstructed the soft proton flare filtering for PN (espfilt)
  - with manual checking of all 6241 public obsids
- Used OMNIdata for the solar wind (multi-mission)
  - more complete coverage than ACE
  - more uniform calibration
- Used TS05 model in geopack for  $\vec{B}$
- Used Shue (1998) model for magnetopause
- Used Bennet et al (1997) model for bowshock
  
- Determined flare incidence rate (“flare fraction”) as function
  - s/c distance from earth/current distance to MP (same  $\mathcal{L}$ )
    - as a function of magnetic geometry
  - angle of look direction from velocity
  - angle of look direction from  $\vec{B}$

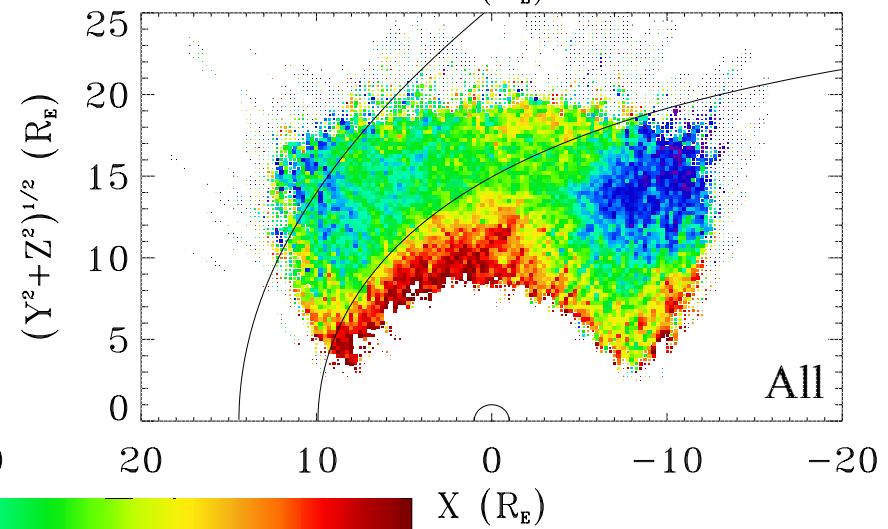
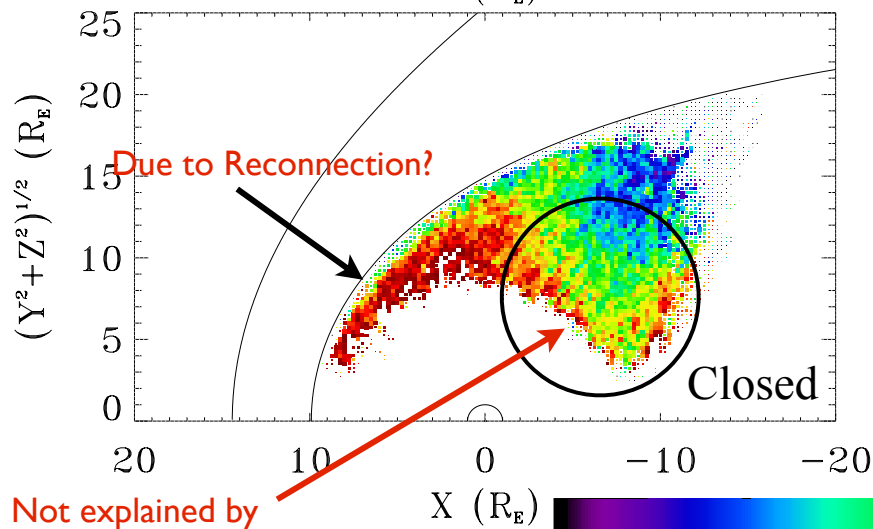
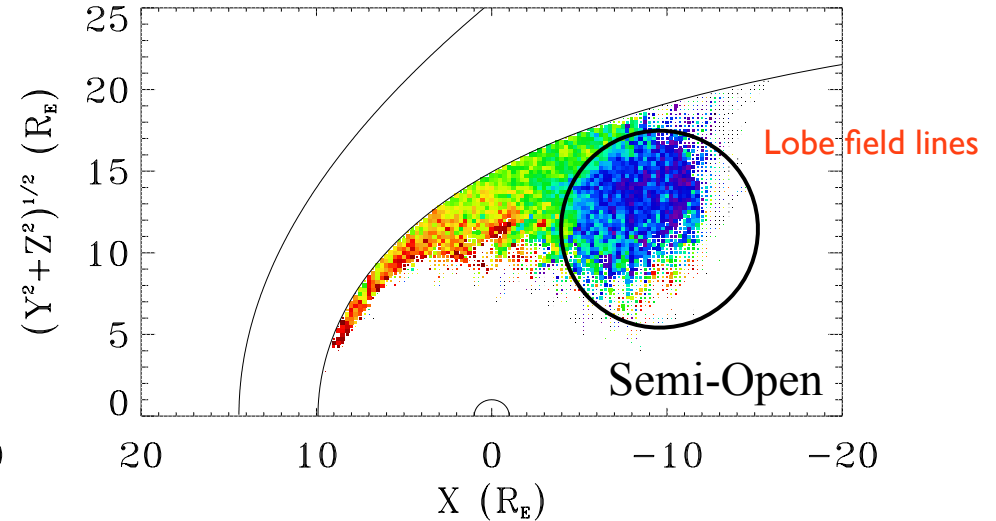
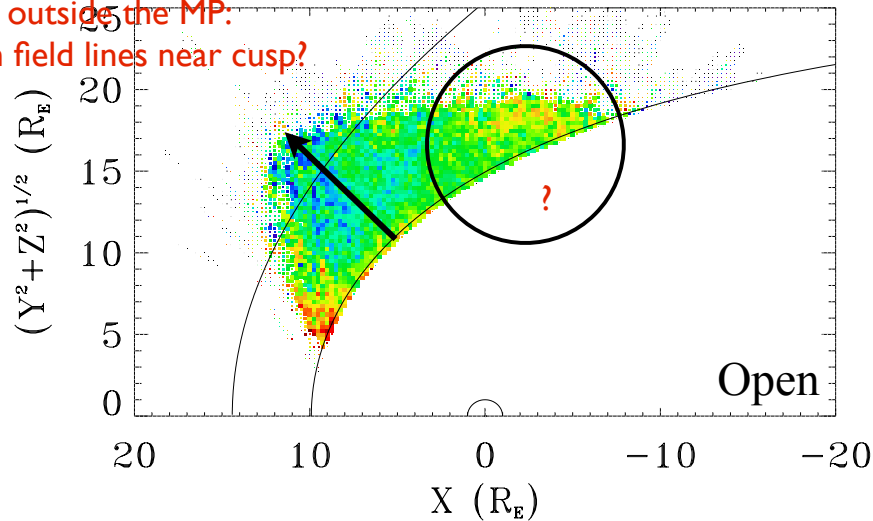
# Where are the proton flares?



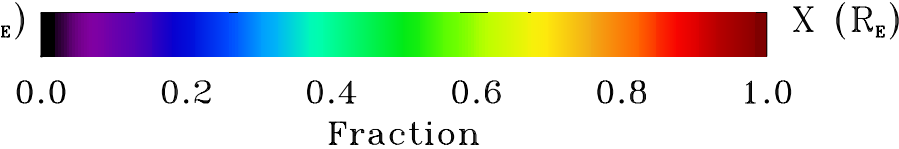
The flare fraction is the highest on closed field lines.  
The “hot zone” is just inside the magnetopause.

# Where are the proton flares?

Gradient in flare fraction  
outside the MP:  
open field lines near cusp?

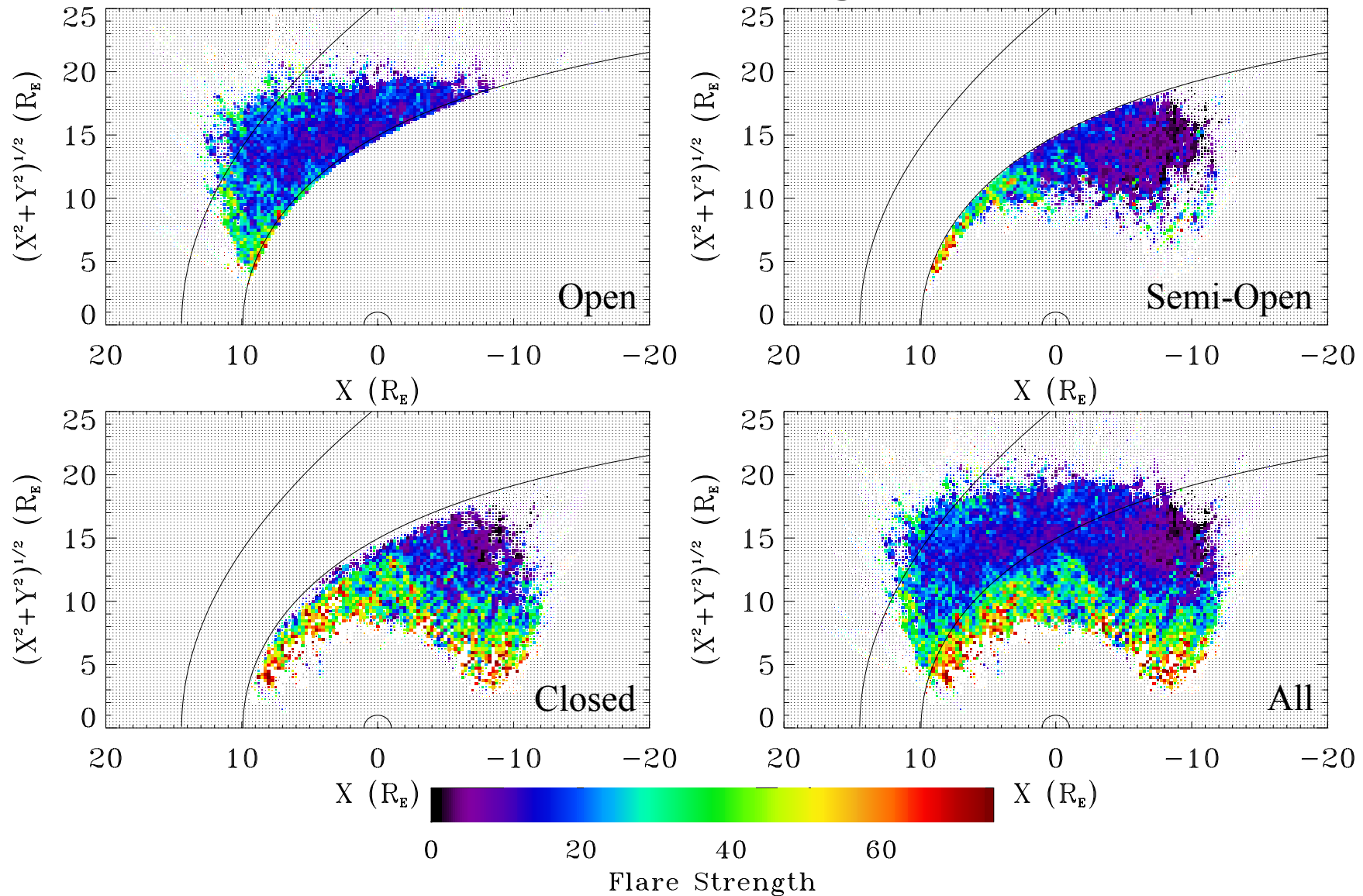


Not explained by  
reconnection



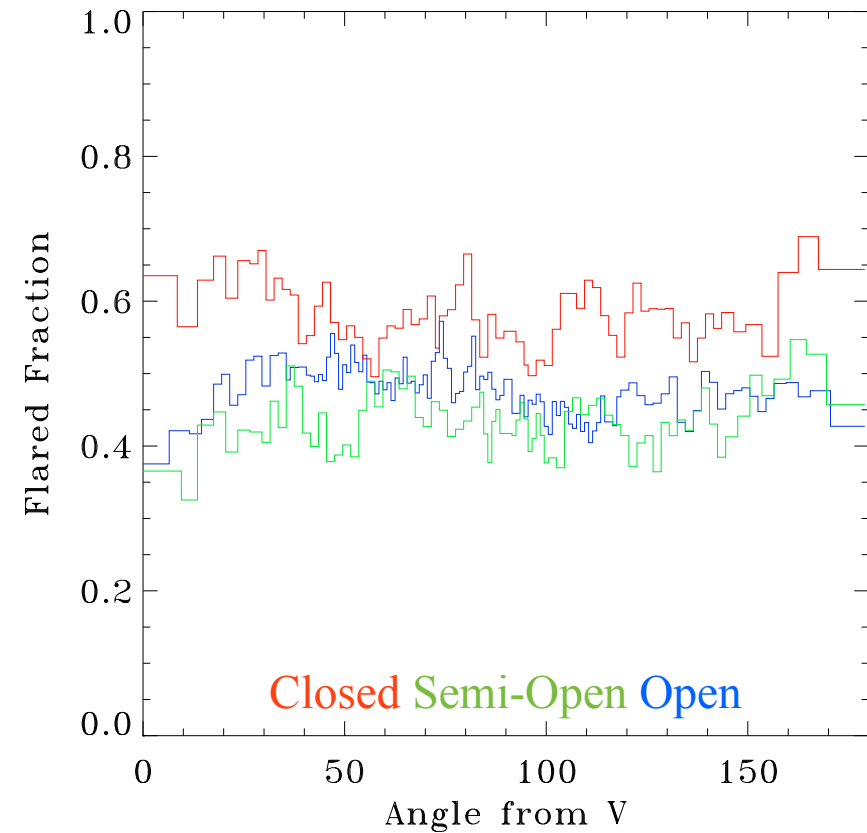
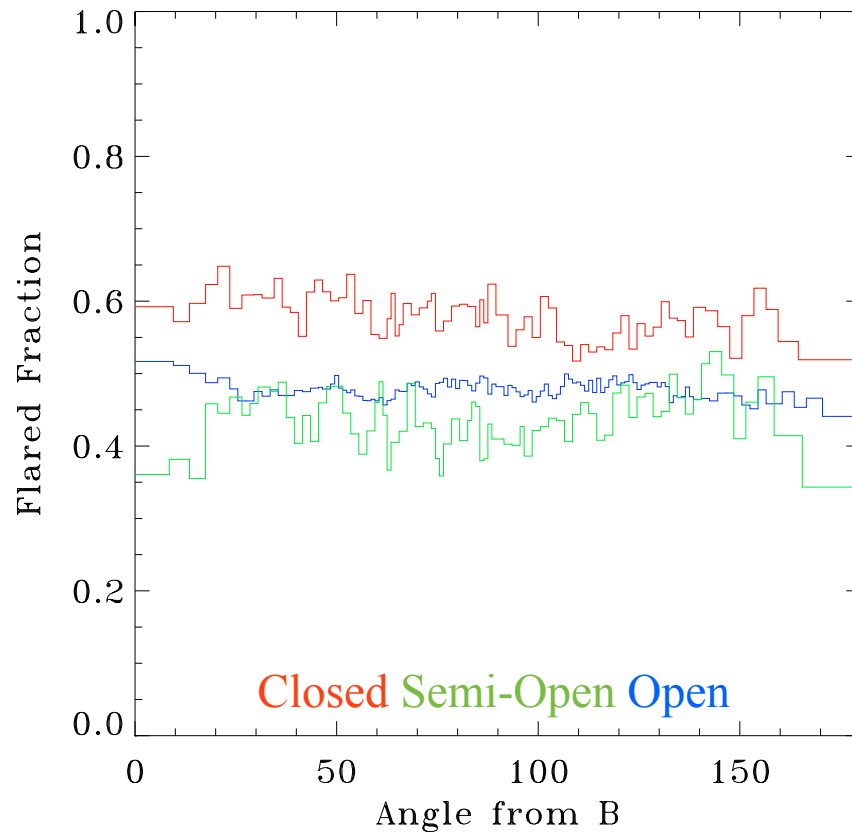
Caveat: the placement of the magnetopause is uncertain, so the interpretation of events near the magnetopause is equivocal.

# Where are the strongest flares?



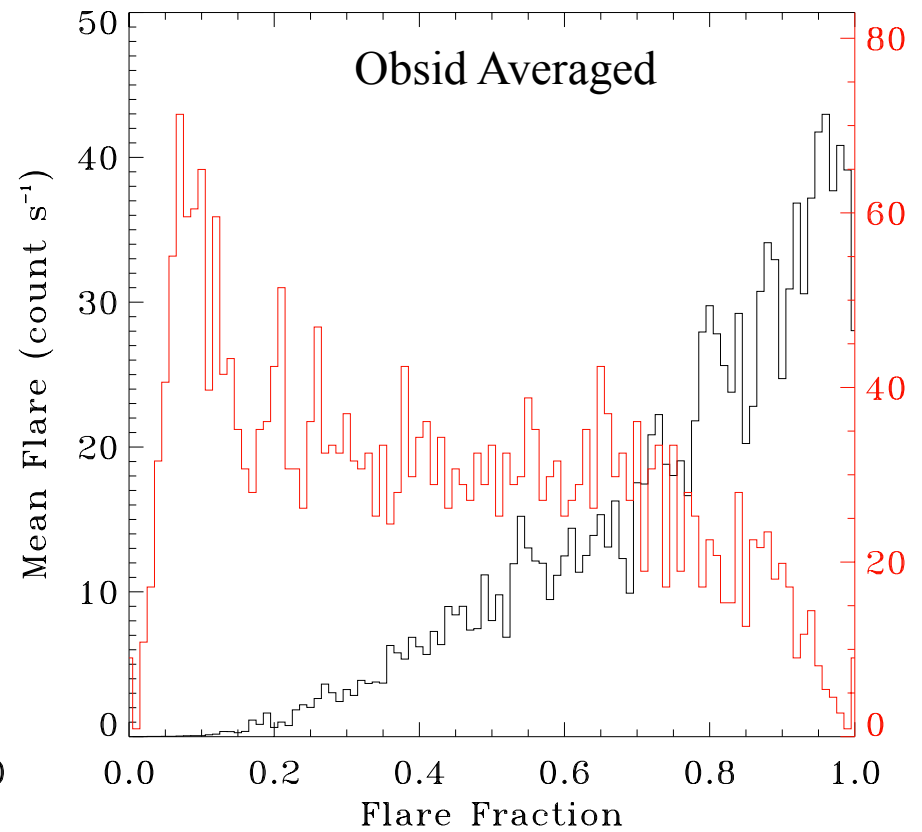
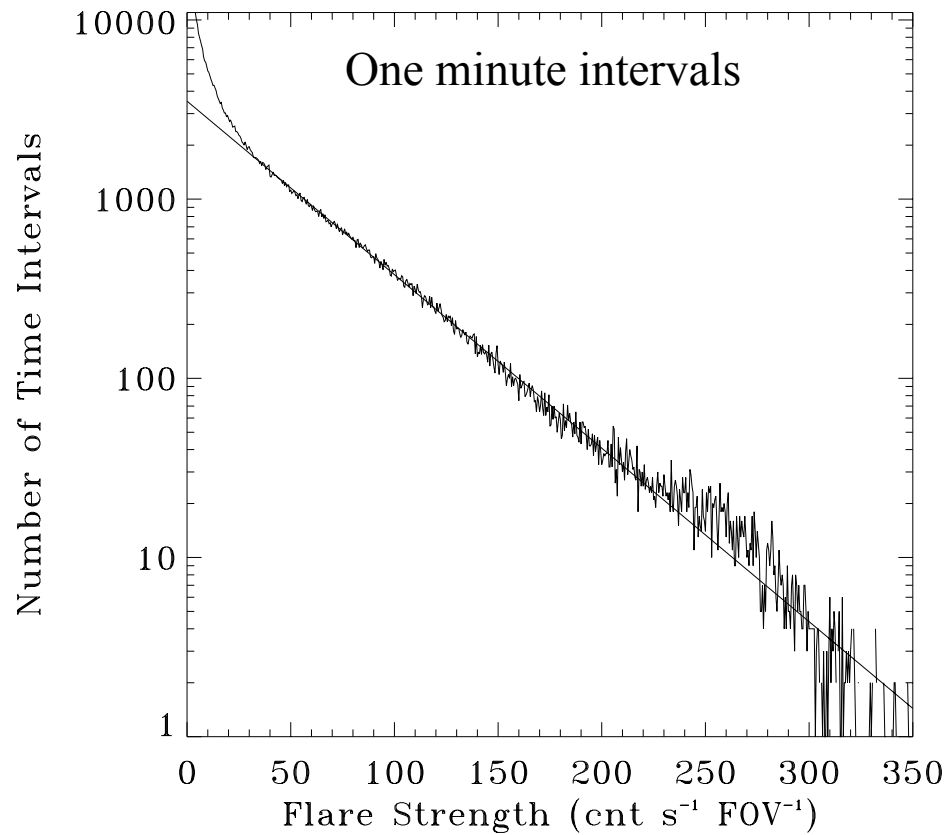
As expected, strongest flares are closest to the Earth.  
(Some confusion with particle belts?)

# Dependence on Look-Direction?



No strong trends in flare fraction seen as a function of the angle between the look direction and  $\vec{B}$  (or  $\vec{V}$ ).

# And the Usual Statistics



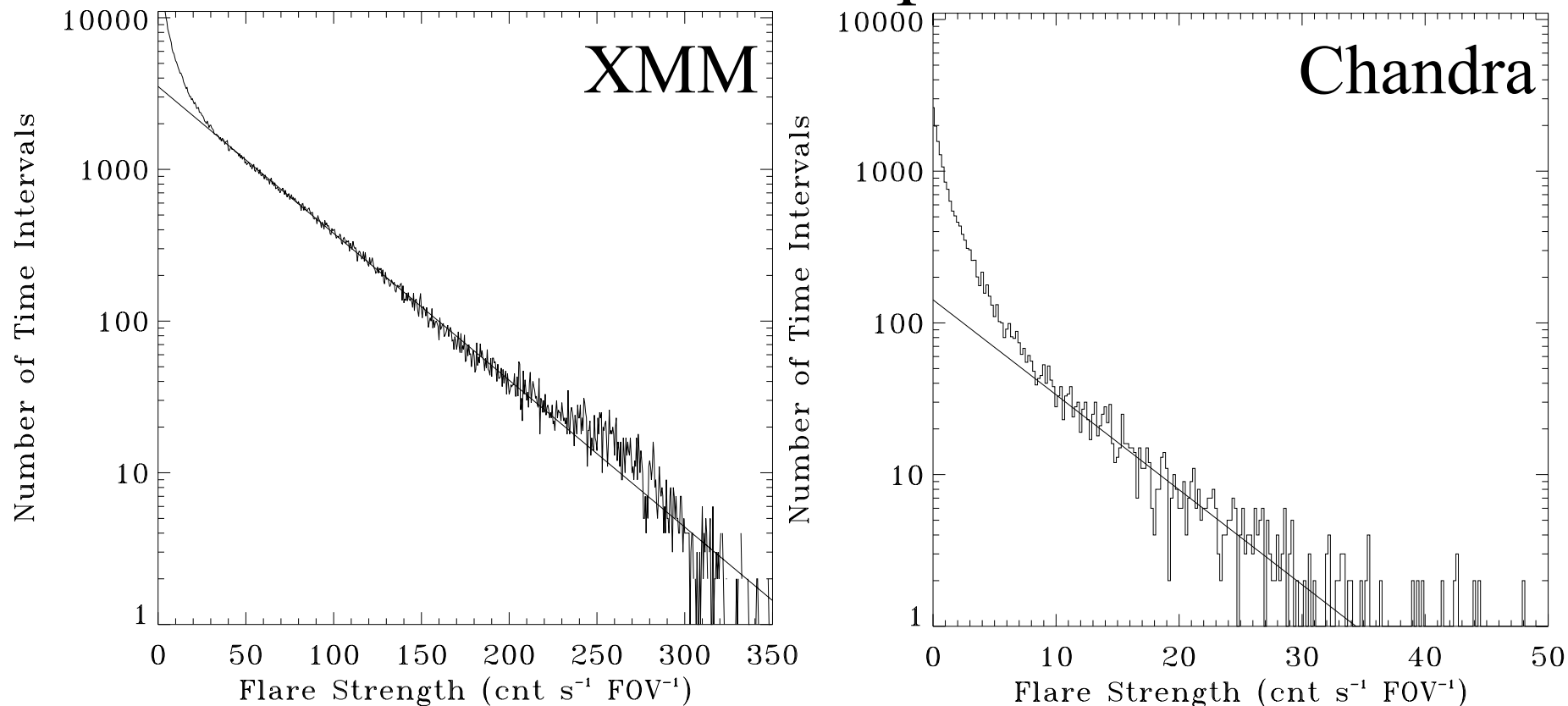


# Why Not Chandra?

Roughly 51% of XMM time is flared, but only 8% for Chandra. Several suggestions have been made for the difference:

- Different orbits
  - Chandra,  $i=28.5$ ,  $a=25.4 R_E$ ,  $e=0.80$  (launch)
  - XMM,  $i=-40.0$ ,  $a=21.0 R_E$ ,  $e=0.79$  (launch)
- Different mirror/optical train efficiencies
  - At 100 keV ACIS/MOS~2 (Nartallo et al 2000)
  - At 200 keV ACIS/MOS~3
  - $\eta \equiv \Omega A_{\text{source}} N_{\text{detect}} / (4\pi A_{\text{detect}} N_{\text{incident}})$
- Different detector sizes
  - Chandra S3,  $6.03 \text{ cm}^2$ ,  $70.5 \text{ arcmin}^2$
  - XMM PN,  $30 \text{ cm}^2$ ,  $706 \text{ arcmin}^2$
- Different detector designs
  - ???

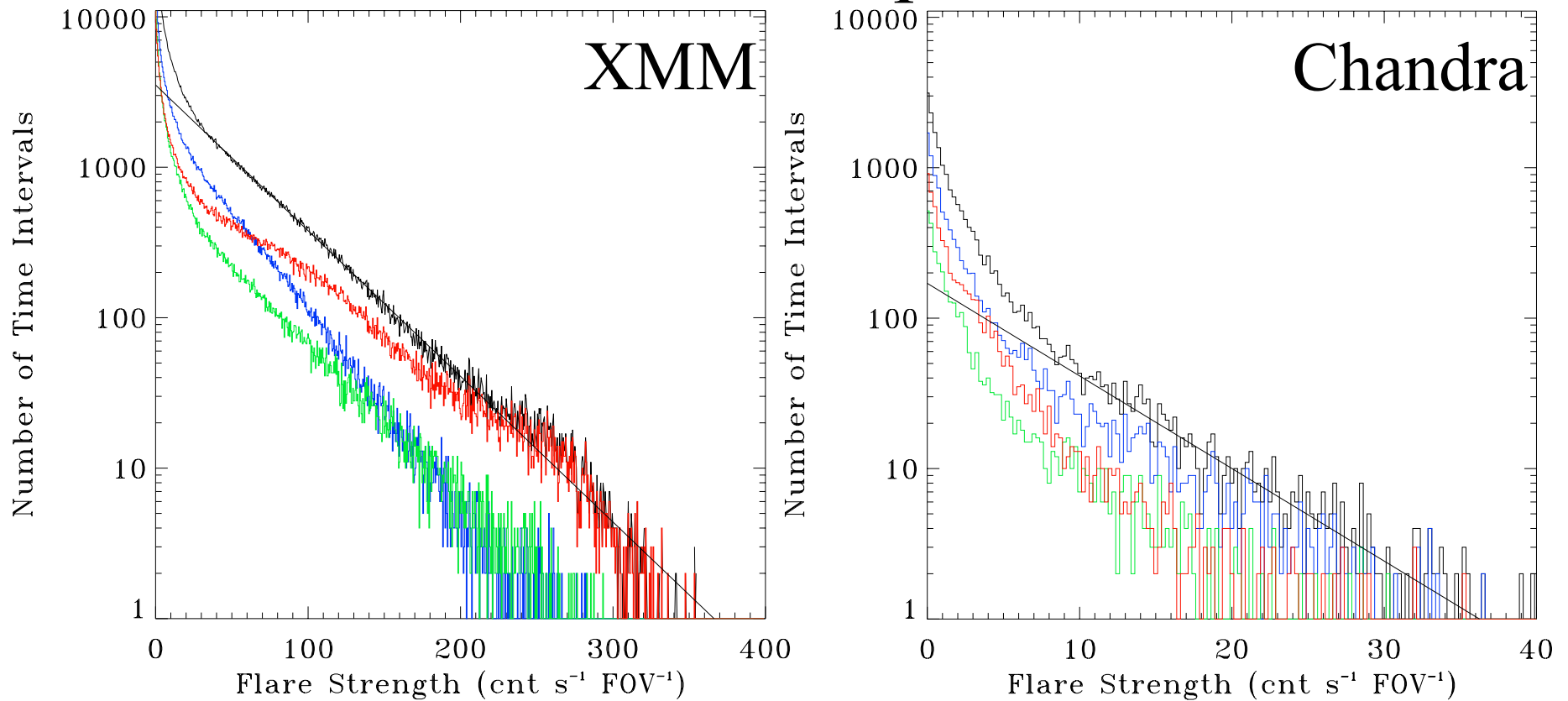
# Chandra Comparison



Maximum flare strength for Chandra is  $\sim 1/10$  that of XMM

- makes it more difficult detect flares at low levels
- since low amplitude flares are more common
  - can significantly reduce the number of flares

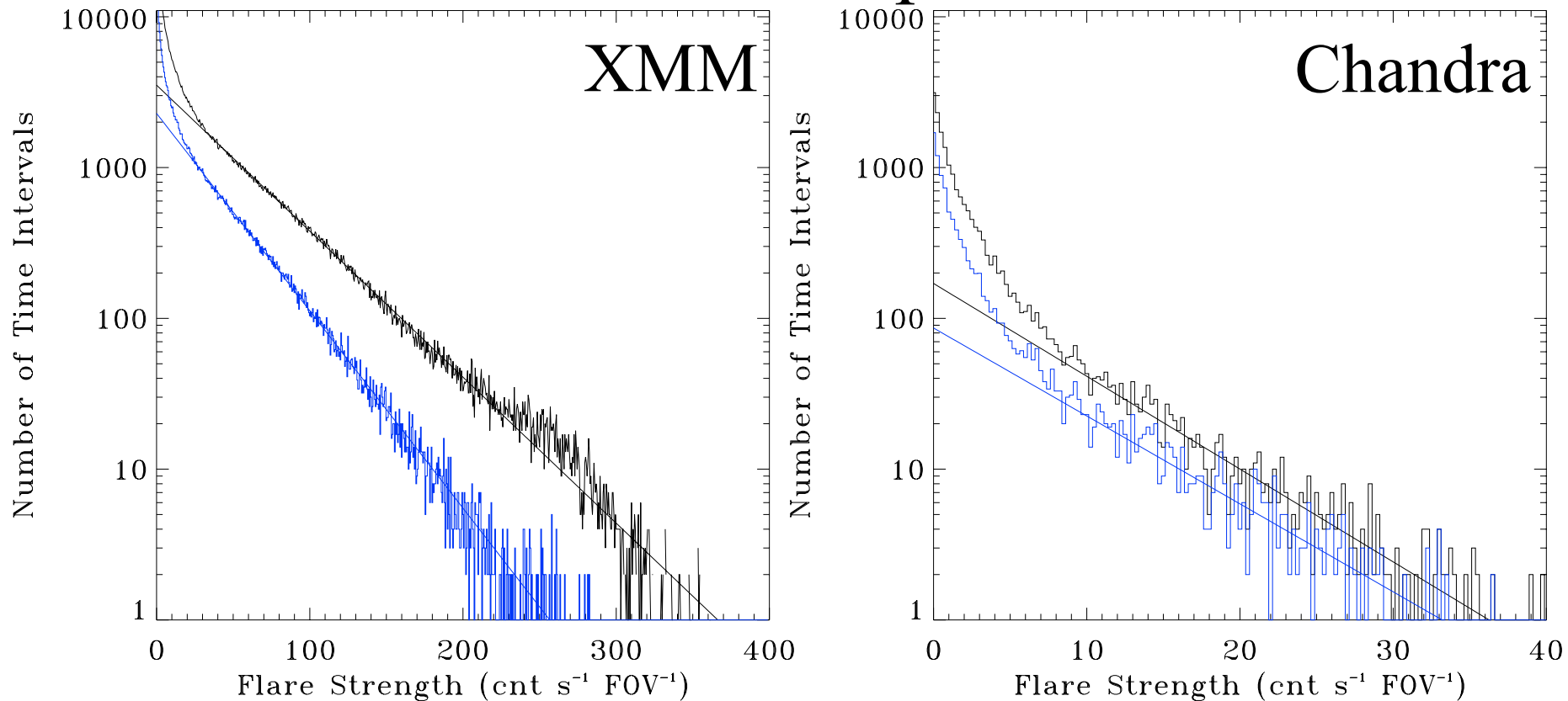
# Chandra Comparison



Comparing the total distribution is a bit unfair

- Divide the distribution by local  $\vec{B}$  geometry
- XMM shows broader variety of behaviors

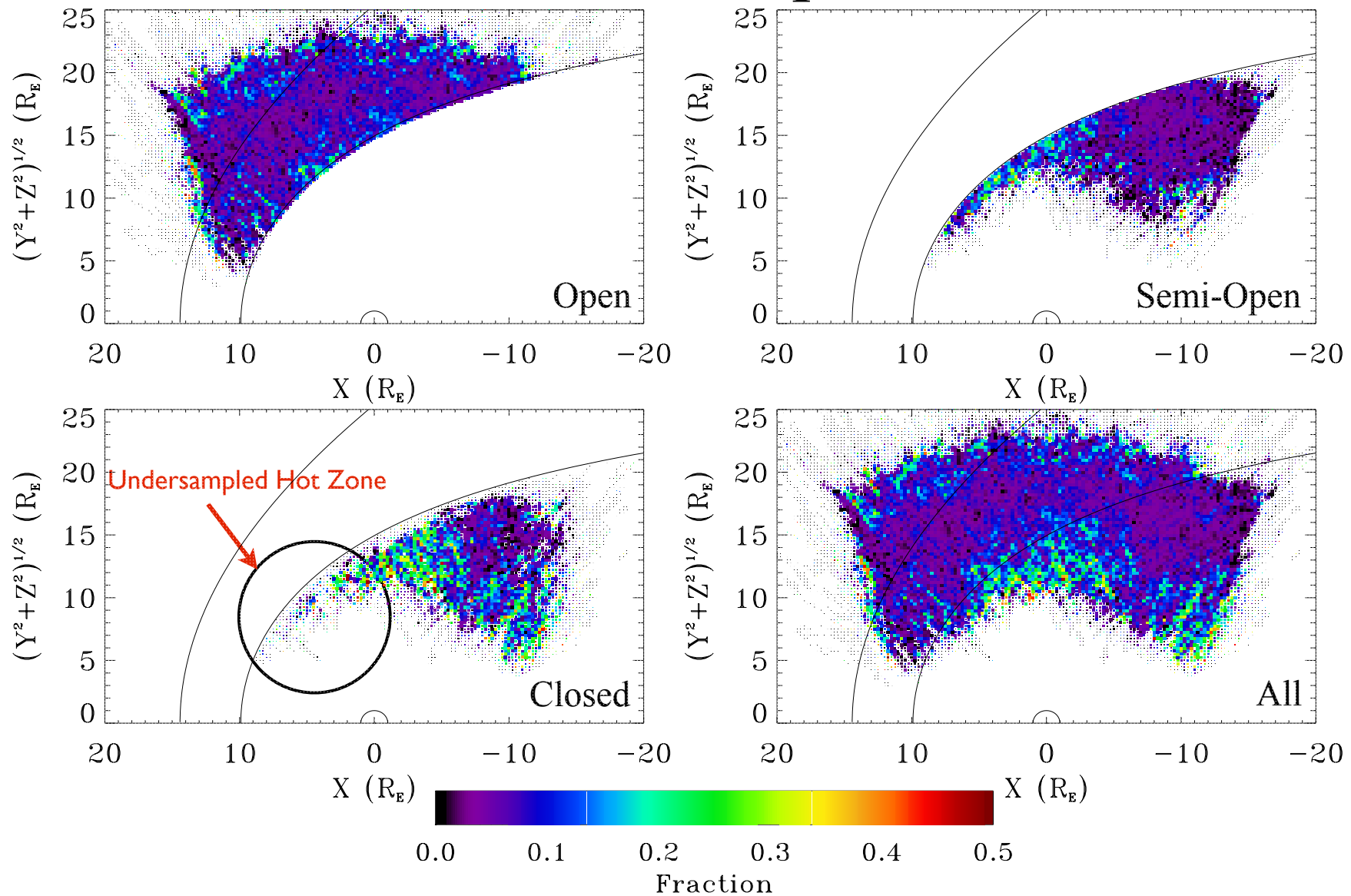
# Chandra Comparison



Maximum flare strength for Chandra is  $\sim 1/8$  that of XMM

- comparing only flares on open field lines
- slopes dissimilar (not clear why)

# Chandra Comparison



Same flare fraction pattern as XMM (but lower amplitude)  
Chandra does not spend as much time (on) in the “hot-zone”

# Chandra Comparison

The “hot zone” is just inside the magnetosheath and has

- highest incidence of flares
- strongest flares

Two reasons why the Chandra is lower:

- it does not observe as much in the “hot zone”
- over-all response to flares is lower so less obvious
- not obvious why the response is lower

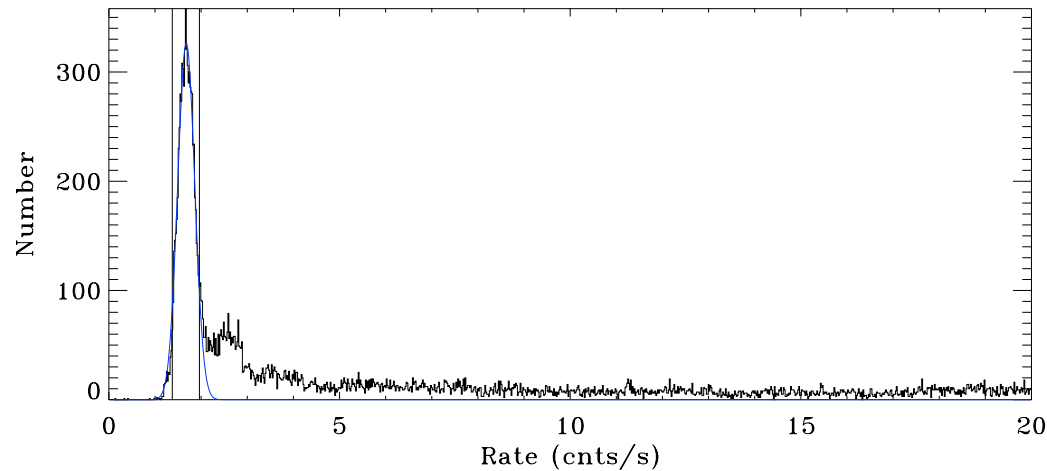
**Quod Erat Demonstrandum**

XYZ

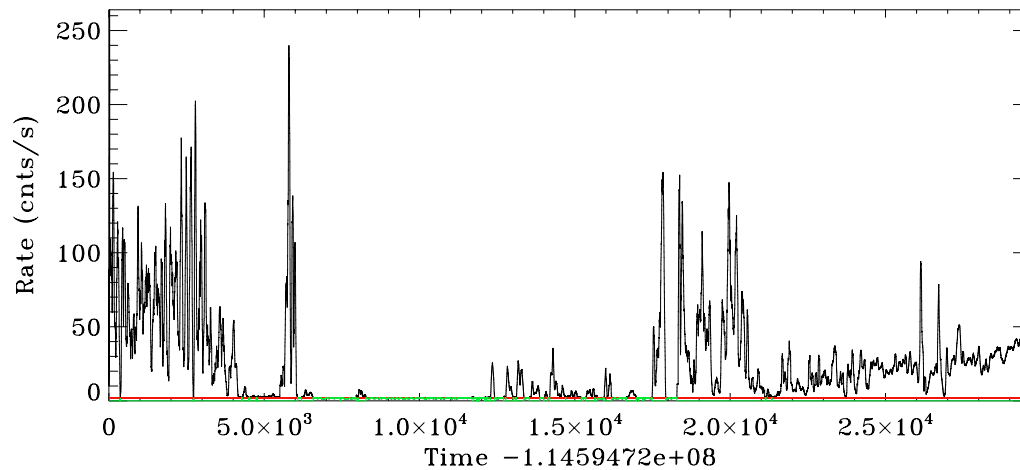


# Determining the Flare Times/Rates

0000110101

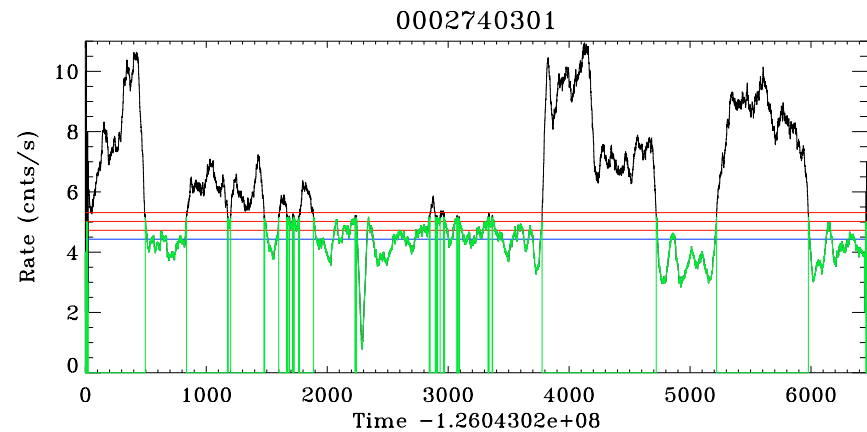
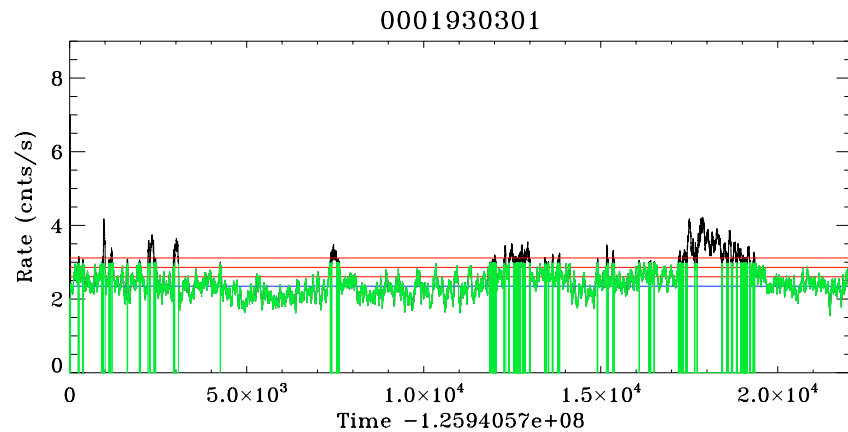
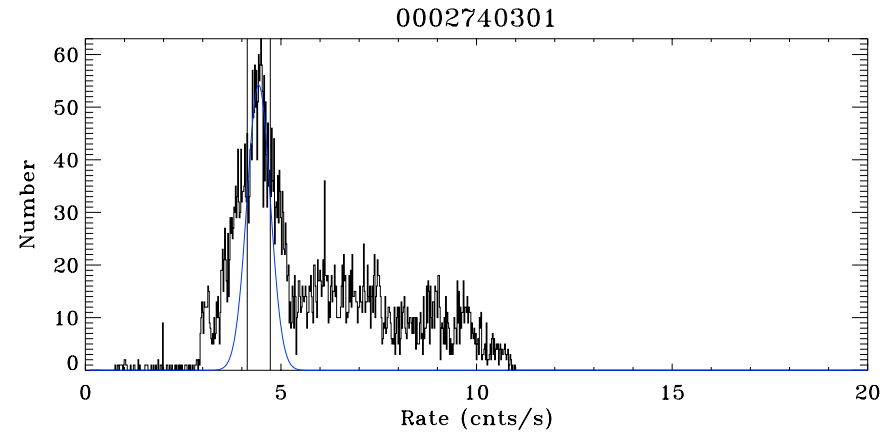
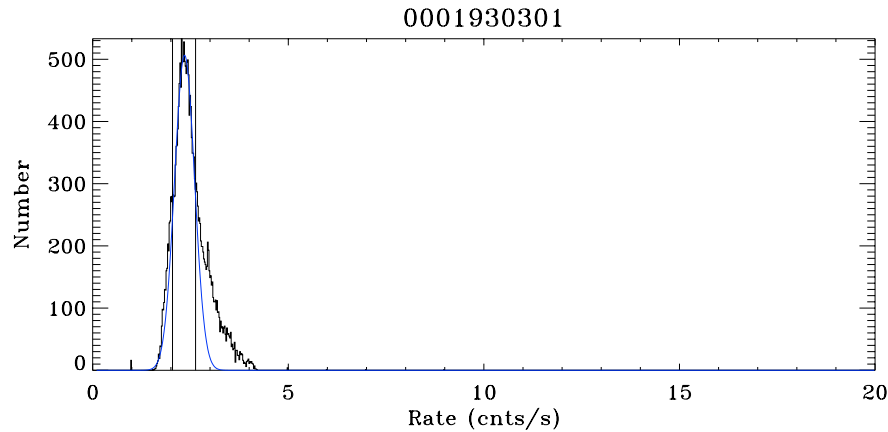


0000110101



Create a histogram of the light-curve,  
Fit a Gaussian to the lowcount-rate peak  
Set threshold over which emission is considered “flare”  $\sim 3\sigma$

# Determining Flare Times/Rates

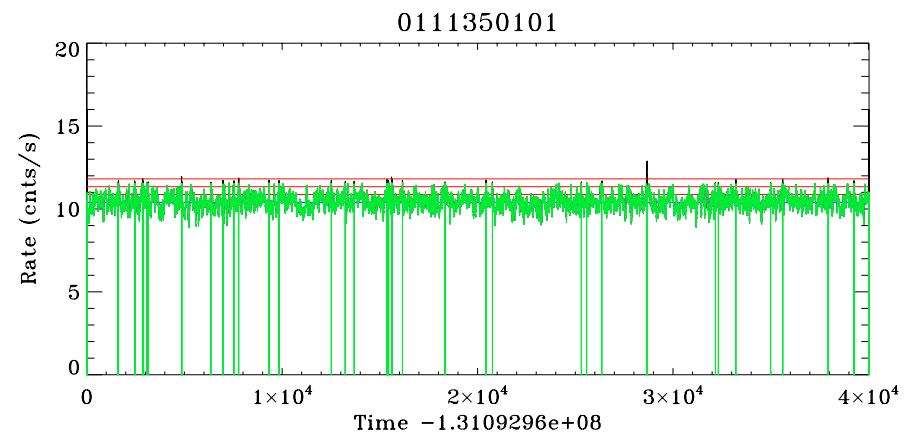
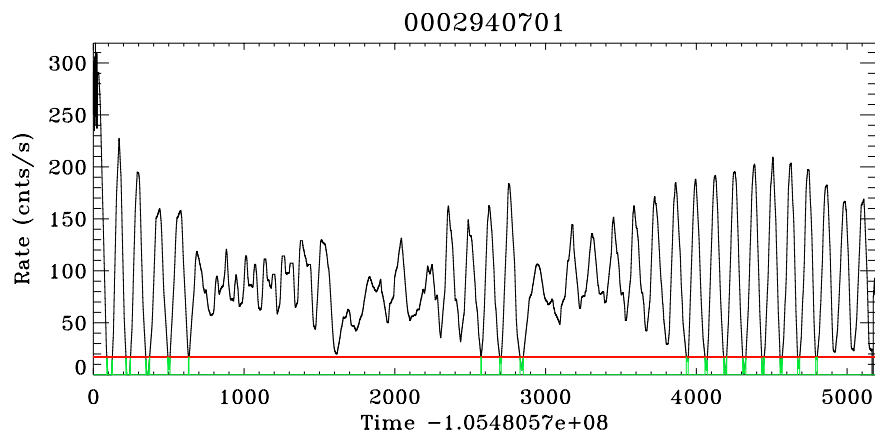
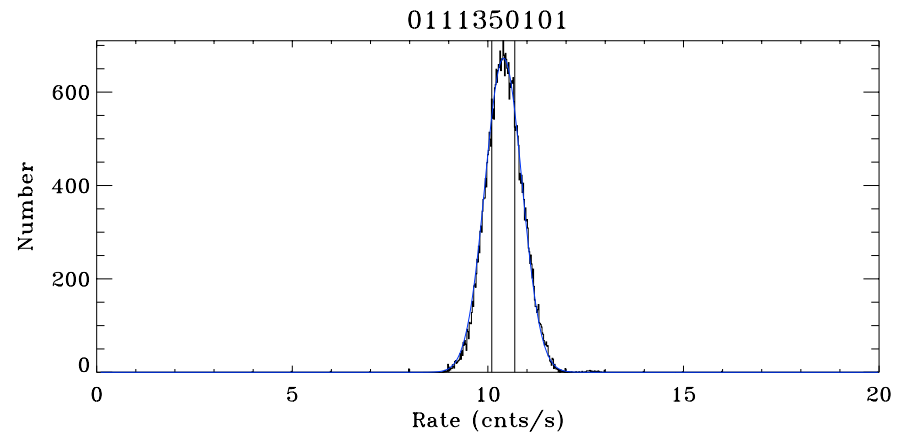
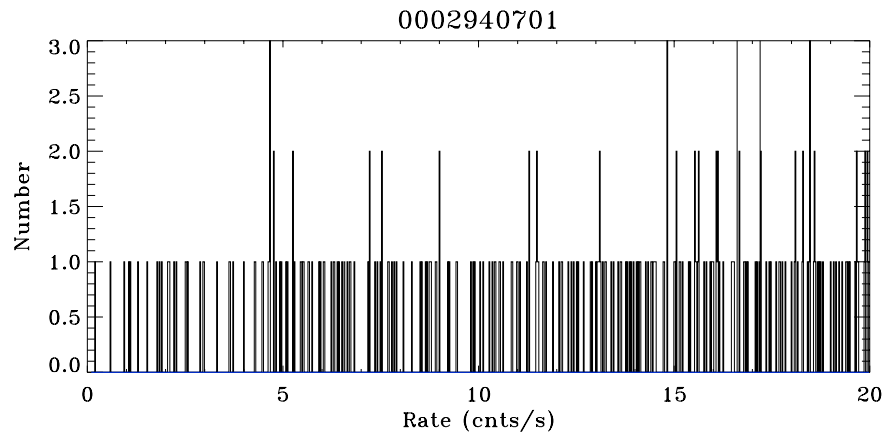


Fully automated fitting doesn't always work:

By eye categorization as good, bad, or indifferent

- good: can get flare intervals and strengths
- indifferent: can get flare intervals but not strengths
- bad: can't get info about flares

# Determining Flare Times/Rates



Fully automated fitting doesn't always work:

By eye categorization as good, bad, or indifferent

- good: can get flare intervals and strengths
- indifferent: can get flare intervals but not strengths
- bad: can't get info about flares

XYZ